BNL-NUREG -23121
INFORMAL REPORT

FAILURE ANALYSIS OF STEAM GENERATOR TUBES WITH DENTED AND WASTAGE CONFIGURATIONS

MARCH 1978

M. REICH, S. PRACHUKTAM, D. GARDNER
H. GORADIA, P. BEZLER, K. KAO

DEPARTMENT OF NUCLEAR ENERGY BROOKHAVEN NATIONAL LABORATORY
UPTON, NEW YORK 11973

Prepared for the U.S. Nuclear Regulatory Commission
Office of Nuclear Reactor Regulation
Contract No. EY-76-C-02-0016

BNL-NUREG-23121
INFORMAL REPORT

FAILURE ANALYSIS OF STEAM GENERATOR TUBES WITH DENTED AND WASTAGE CONFIGURATIONS*

By

M. Reich, S. Prachuktam, D. Gardner, H. Goradia, P. Bezler, K. Kao
Structural Analysis Group
Department of Nuclear Energy
Brookhaven National Laboratory
Upton, New York 11973

March 1978

*Work performed under the auspices of the United Stated Nuclear Regulatory Commission.

TABLE OF CONTENTS

ABSTRACT

The occurrence of PWR steam generator tube cracking, denting, and wastage has been reported in the recent literature (1-5). As indicated by its title, this paper concerns itself with the inelastic structural response of the tubes that result from various assumed monotonic as well as cyclic loading conditions, which ultimately could lead to the tube failure.

LIST OF FIGURES

LIST OF FIGURES (CONT'D)

LIST OF FIGURES (CONT'D)

LIST OF TABLES

Introduction

Typical PWR steam generator units contain thousands of tubes that are guided and positioned along their lengths by support plates of various design. A number of steam generator tube problems, such as the formation of wastages and cracks on the outer surfaces of the tubes, have been reported in the literature[1-2]. Although initial clearance in the support plates of particular types of steam generators are provided to allow for sliding of the steam generator tubes under all contemplated operating conditions, there are occasions, as reported in the recent literature,[3-5] when corrosion or so-called "crud" product build-up in the clearance gaps results in tube seizure and ultimate failure. This latter phenomena has mainly been experienced in Westinghouse steam generators.

Since the steam generator tubes serve as the primary containment of the reactor coolant, it is important to better understand the margins of safety inherent in the degraded tubes. In accordance with the Regulatory Guide 1.121,[6] tubes with detected part-thru wall cracks should not be stressed beyond the elastic range of the tube material, and tubes with part-thru wall cracks, wastages, or combinations of these shall have a factor of safety against failure by bursting of not less than three at any location. These criteria apply for the full range of normal operating conditions. In addition, margins of safety against tube failure under postulated accidents should be consistent with the margin of safety determined by the stress limits specified in NB-3225 of Section III of the ASME Boiler and Pressure Vessel Code.

This paper concerns itself with the elastic structural response of steam generator tubes having various degradations. Specifically, nonlinear finite element analysis methods using large displacement formulations were carried out to determine burst pressures for tubes containing elliptical

wastages and part-thru circumferential cracks. For tubes "seized" in the support plate holes, operational cyclic pressure and temperature loadings were evaluated for inelastic ratcheting responses. The behavior of tubes containing longitudinal cracks is presented in detail in a separate report[7].

Analysis Methods and Features

All analyses to be presented were carried out with the Nonlinear Finite Analysis Program(NFAP)[8]. This general purpose program contains two-dimensional plane, and axisymmetric, as well as three-dimensional isoparametric elements that can be applied to problems involving nonlinear material behavior and large deformations. Other features of the code include direct pressure inputs for the isoparametric elements, scaling of the initial yield load, automatic load increment adjustments for convergent nonlinear solutions, pressure-geometry dependency, an automatic bandwidth reduction scheme, an out-of-core solution solver, and a graphic-grid stress-strain output, etc. The numercial accuracy of the program was investigated and checked with known benchmark problems[8].

Analysis of Results for Tubes with Elliptical Wastages

Figure 1 depicts the four-layer, 360 eight-node, plane strain finite element grid used to model the tubes containing the elliptical wastages. Essentially, this is a two-dimensional approximation of a real tube with an elliptical wastage whose major axis is longitudinally oriented (See Figure 6). The tube analyzed was a 0.750 in. O.D. (1.905 cm) x 0.048 in. (0.122 cm) wall—Inconel 600 with an elliptical wastage having a major axis 1.50 inches long (3.810 cm) and a minor axis of 0.750 inches (1.905 cm) long. For the analysis, wastage depths were assumed to vary from 50 percent to 90 percent of the original wall thickness.

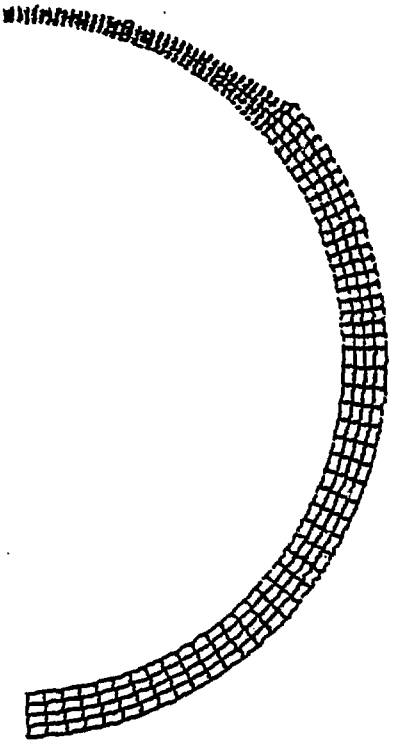

FIGURE 1

TYPICAL FINITE ELEMENT GRID OF THE WASTAGE TUBES

Figures 2A-2F and 3A-3F show the calculated results for the 50, 60, 65, 70 80, and 90 percent depth wastages for both the internal and external pressure loadings. Figures 2A through 2F depict the original (shown with dotted line) and deformed shapes for the above-mentioned cases when subjected to internal pressure at the point where the tubes cannot sustain any additional load increments. Figures 3A through 3F show the corresponding results for the external pressure loadings. For the sake of clarity, a scale factor of 10 was applied to the calculated results used in depicting the deformed shapes shown in the above-mentioned figures.

Table I summarizes the results for the internal pressure cases. Values are listed for the failure pressure, effective stress, effective strain, and a strain limit failure criteria based on a triaxiality correction factor, described in the literature[9,10]. The results shown in the table correspond to a condition of plastic instability in that the tube cannot sustain any additional loading. Preliminary calculations indicate that a failure condition corresponding to an ultimate loss of area could be reached for some cases. However, subsequent investigations indicated that the preliminary results were in error. It seems that this failure condition would occur either at the listed pressure or a slightly higher pressure.

Table II shows the results obtained for the external pressure cases. Values are listed for the pressure corresponding to the elastic collapse and the plastic instability. The elastic collapse pressure is defined as the external pressure at the time when the first element in the tube yields, while the plastic instability pressure is the external pressure when the structure cannot sustain any additional load. Figures 4 and 5 graphically summarize the results for the two-dimensional internal and external pressure cases discussed above.

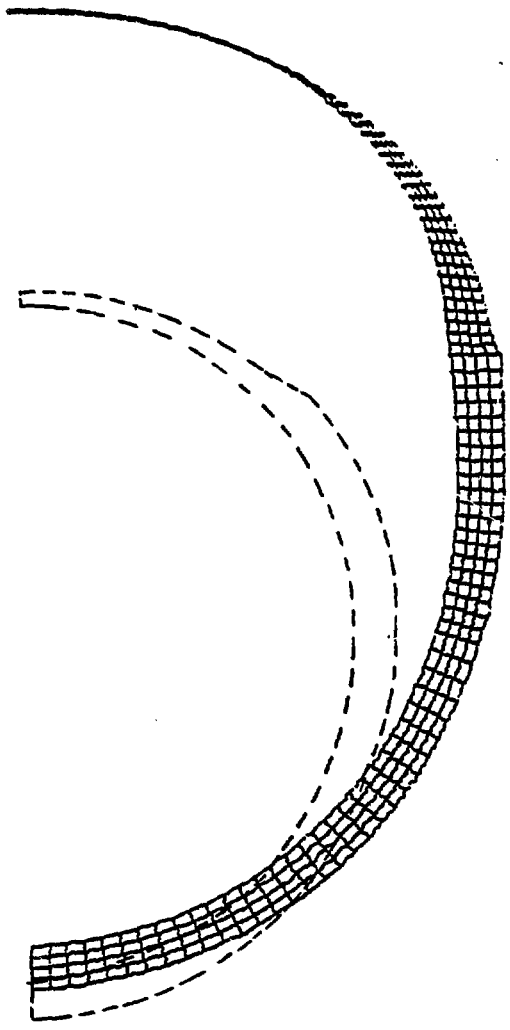

FIGURE 2A

CROSS-SECTION OF THE 50% WASTAGE TUBE AT 4976 PSI—INTERNAL PRESSURE CONDITION

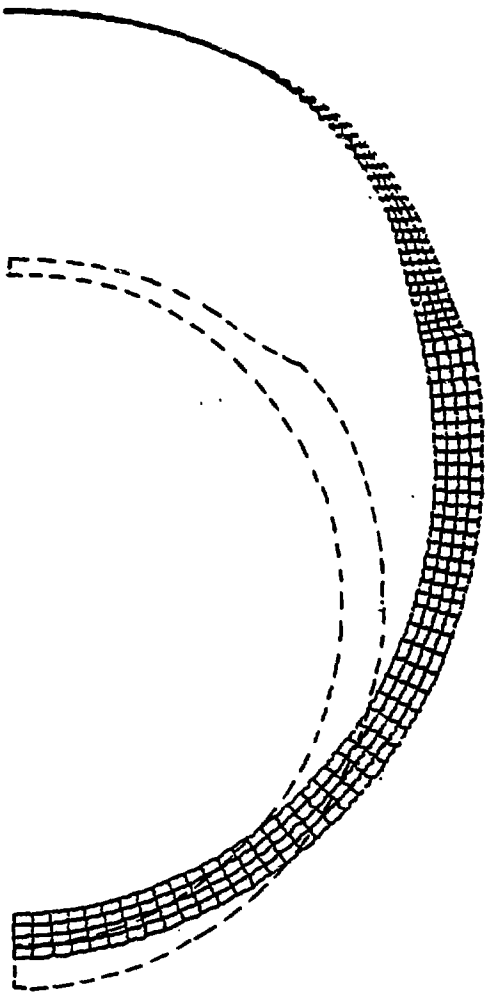

FIGURE 2B

CROSS-SECTION OF THE 60Z WASTAGE TUBE AT 4022 PSI—INTERNAL PRESSURE CONDITION

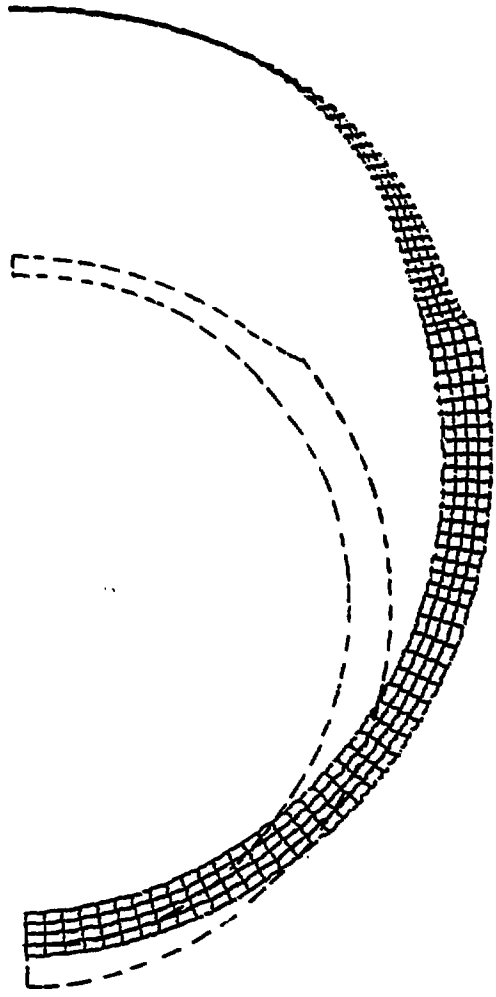

FIGURE 2C

CROSS-SECTION OF THE 65% WASTAGE TUBE AT 3567 PSI—INTERNAL PRESSURE CONDITION

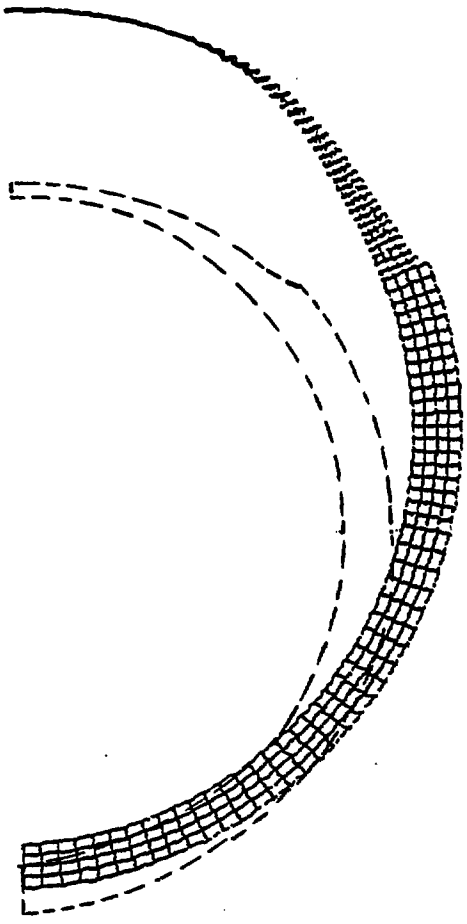

FIGURE 2D

CROSS-SECTION OF THE 70% WASTAGE TUBE AT 2810 PSI--INTERNAL PRESSURE CONDITION

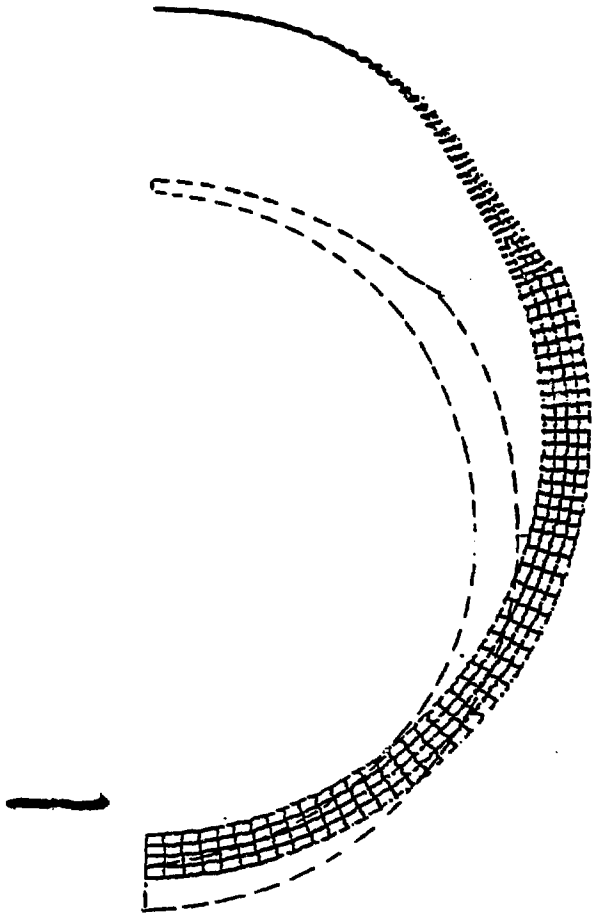

FIGURE 2E

CROSS-SECTION OF THE 80% WASTAGE TUBE AT 2323 PSI--INTERNAL PRESSURE CONDITION

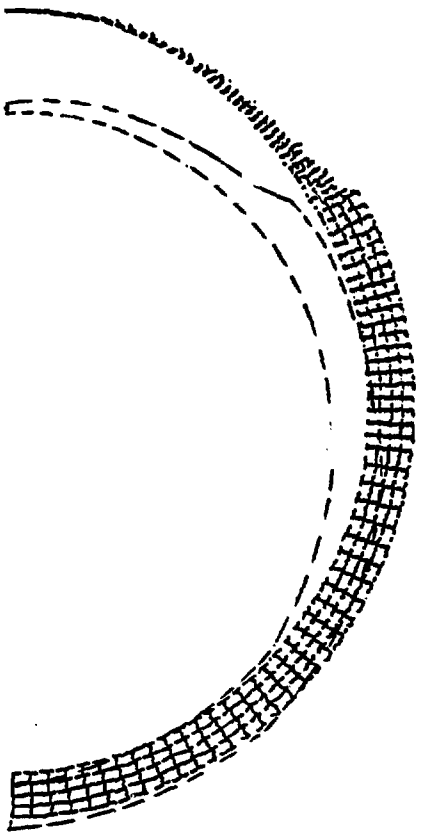

FIGURE 2F

CROSS-SECTION OF THE 90% WASTABE TUBE AT 1907 PSI--INTERNAL PRESSURE CONDITION

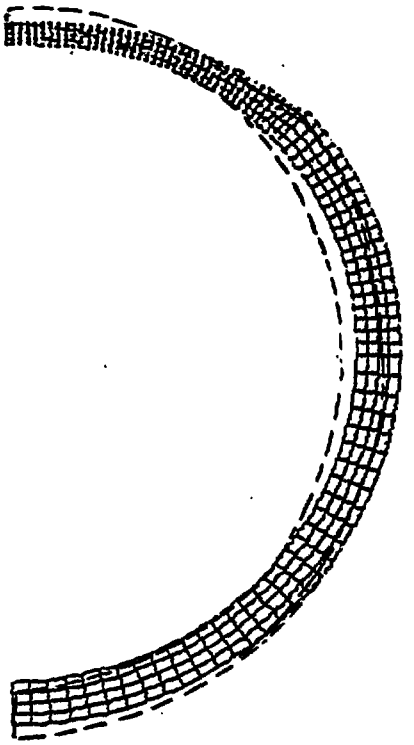

FIGURE 3A

CROSS-SECTION OF THE 50% WASTAGE TUBE AT 2447 PSI--INTERNAL PRESSURE CONDITION

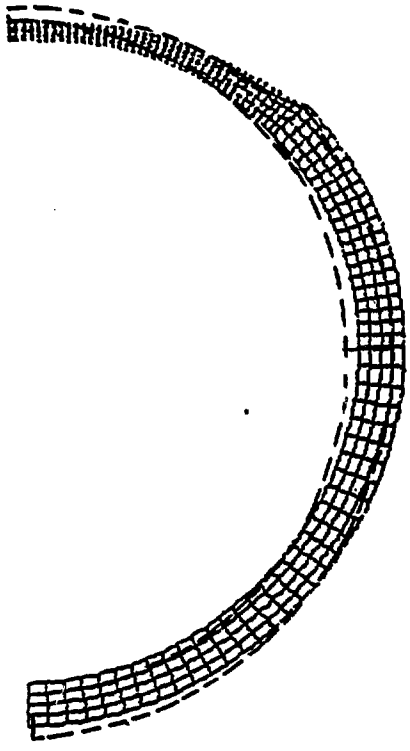

FIGURE 3B

CROSS-SECTION OF THE 60% WASTAGE TUBE AT 1920 PSI--EXTERNAL PRESSURE CONDITION

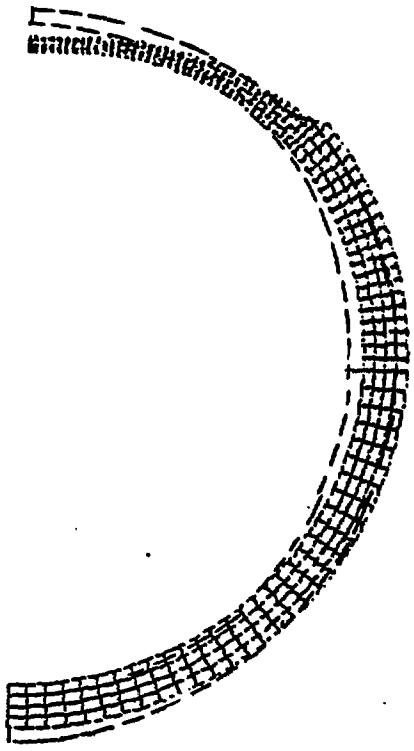

FIGURE 3C

CROSS-SECTION OF THE 65% WASTAGE TUBE AT 1650 PSI--EXTERNAL PRESSURE CONDITION

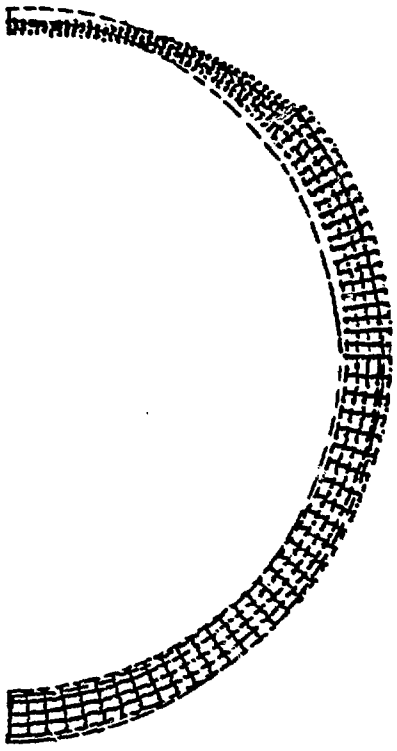

FIGURE 3D

CROSS-SECTION OF THE 70% WASTAGE TUBE AT 1300 PSI--EXTERNAL PRESSURE CONDITION

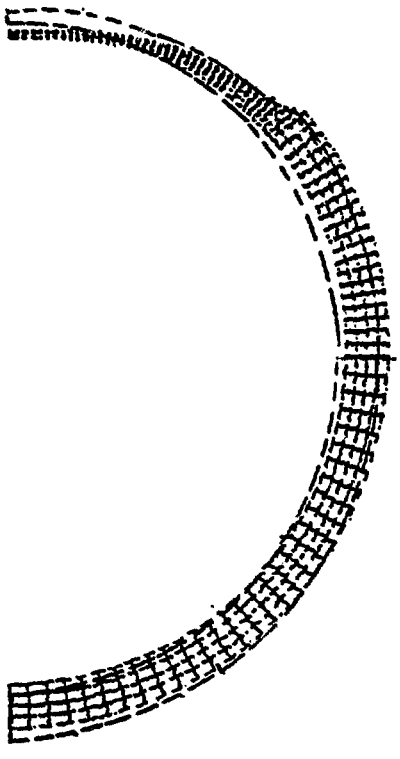

FIGURE 3E

CROSS-SECTION OF THE 80% WASTAGE TUBE AT 850 PSI--EXTERNAL PRESSURE CONDITION

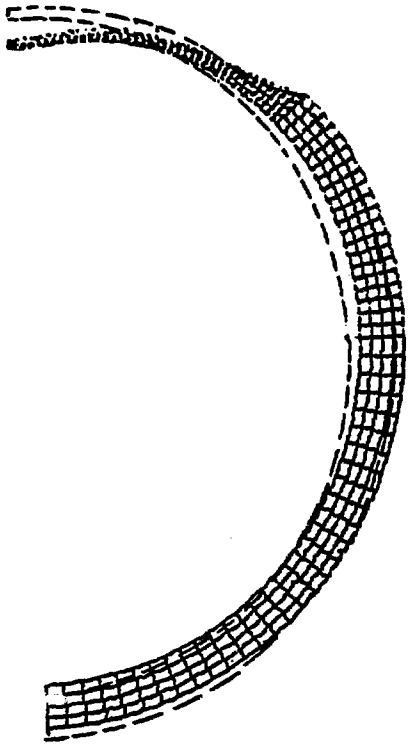

FIGURE 3F

CROSS-SECTION OF THE 90% WASTAGE TUBE AT 751 PSI—EXTERNAL PRESSURE CONDITION

TABLE 1

SUMMARY OF RESULTS OF TWO-DIMENSIONAL WASTED TUBES SUBJECTED TO INTERNAL PRESSURES

% Wastage	Differential Pressure at Failure	Effective Strain %	Strain Limit*%
50	4976	20.4	23.8
60	4022	19.9	22.8
65	3567	20.8	22.4
70	2810	20.7	22.4
80	2323	21.5	22.1
90	2029	20.0	23.1

*Reference (9,10)

$$\varepsilon_p \leq [\ln (1 + E_u) - \sigma_{yd}/E]\, F(TF)$$

$$F(TF) = TF^{-1}[1 - TF^{-1}) (2.940 - 4.545\, TF^{-1})]$$

E_u = Engineering strain at rupture

σ_{yd} = The yield strength

E = Young's modulus

$$TF \text{ (triaxiality factor)} = \frac{\sigma_1 + \sigma_2}{\sigma_{ef}}$$

$$TF = \frac{\sigma_1 + \sigma_2 + \sigma_3}{\sigma_{ef}}$$

where σ_{ef} = Effective stress

TABLE 2

SUMMARY OF THE RESULTS OF TWO-DIMENSIONAL WASTED TUBES SUBJECTED TO EXTERNAL PRESSURE

% Wastage	Differential Pressure at Elastic Collapse	Differential Pressure at at Plastic Instability (at outside surface)
50	1800	2447
60	1440	1920
65	1200	1650
70	914	1300
80	605	850
90	510	751

Internal Failure Pressure for Tubes with
Elliptically* Shaped Wastage Configuration

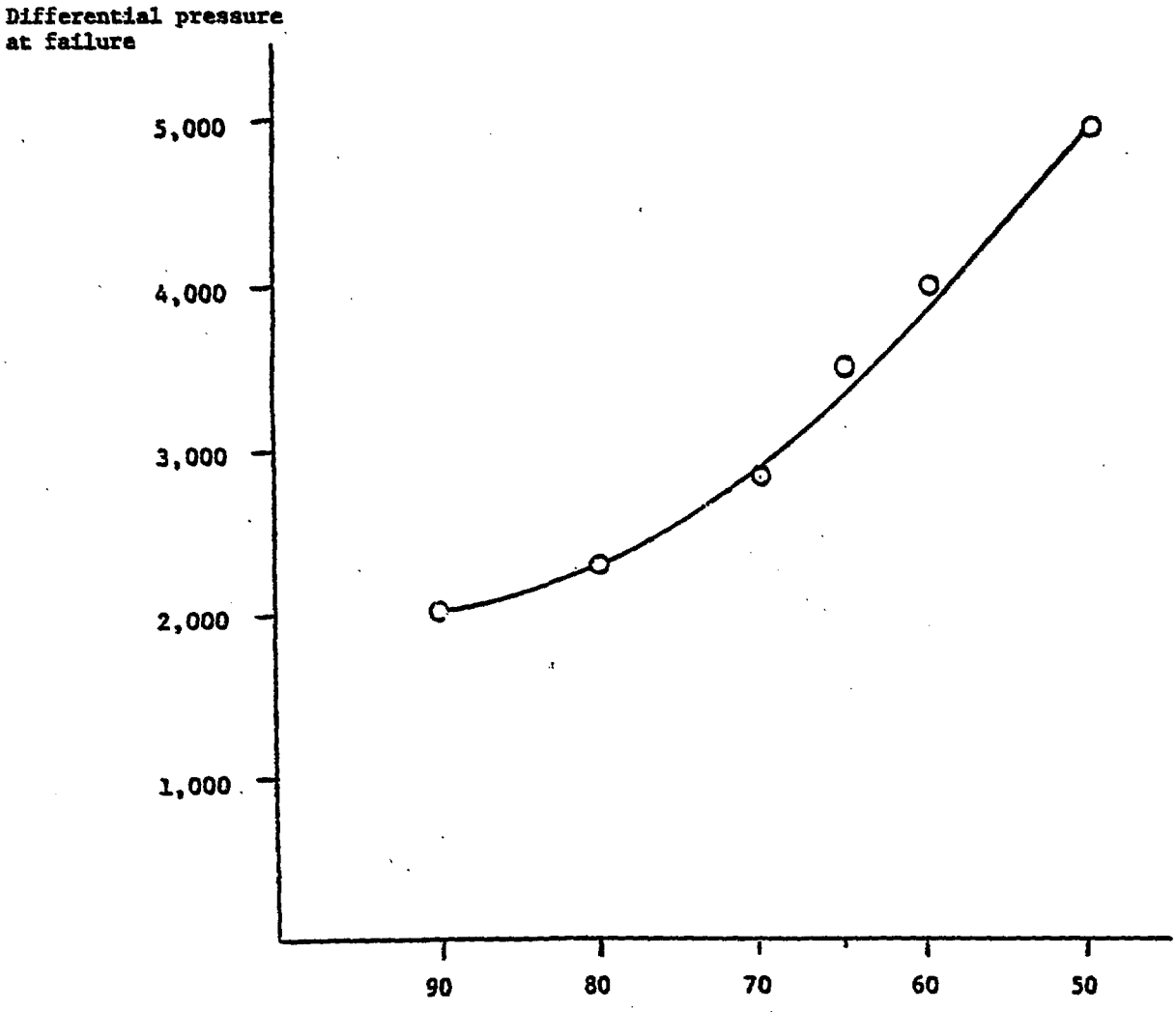

* Major Dia. 1.5 in.
Minor Dia. 0.75 in.

FIGURE 4

External Failure Pressure for Tubes with
Elliptically* Shaped Wastage Configuration

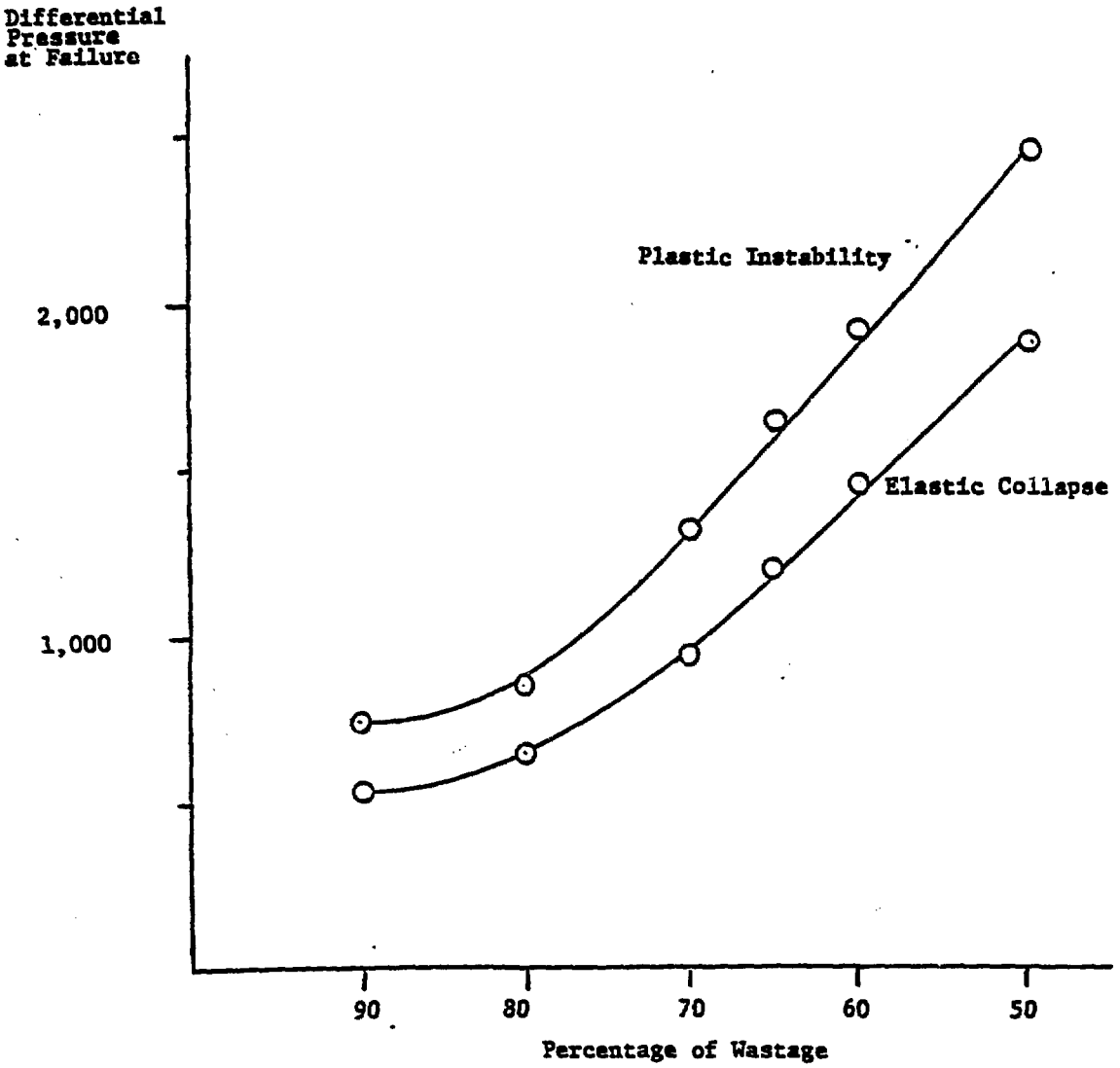

* Major Dia. 1.5 in.
Minor Dia. 0.75 in.

Depth of Wastage

FIGURE 5

EXTERNAL PRESSURE CONDITION

It is to be noted that in the real structure there would be a strengthening effect due to the surrounding intact walls. In order to gain insight into this effect, a three-diemnsional analysis for the elliptical wastage shown in Figure 6 was carried out. The computed effective stress and effective strains vs. internal pressure is depicted graphically in Figure 7. The extent of the plastic zones at failure as determined by the triaxial failure criteria on the inner and outer surfaces of the tubes are shown in Figures 8 and 9, while the radial defections for the center of the wastages are plotted vs. pressure in Figure 10. The burst pressure via the triaxial failure criteria was found to be 2657 psi(18.32 MPa), while computational instability, one of the failure criteria applied for the two-dimensional analysis, did not occur until 2891 psi (19.93 MPa).

Comparing these results with the equivalent two-dimensional failure pressure (2323 psi(16.02 MPa)) indicates a three-dimensional strengthening effect of 12.6 percent or 19.6 percent for the two failure conditions mentioned above. It should be noted that the effective strain at instability (~19.6 percent) is close to that of the two-dimensional case.

While no other three-dimensional analysis for these defect geometries were carried out, some information regarding the strengthening trend may be inferred from results obtained from the three-dimensional analyses carried out for longitudinally cracked tubes.[7] From these studies it seems that for short finite length cracks, the strengthening effect is a function of the crack depth. As the crack depth becomes less, the three-dimensional strengthening effect also becomes less. In regard to crack length, an inverse effect should be expected. For a short length crack maximum strengthening occurs while for a long crack no strengthening should

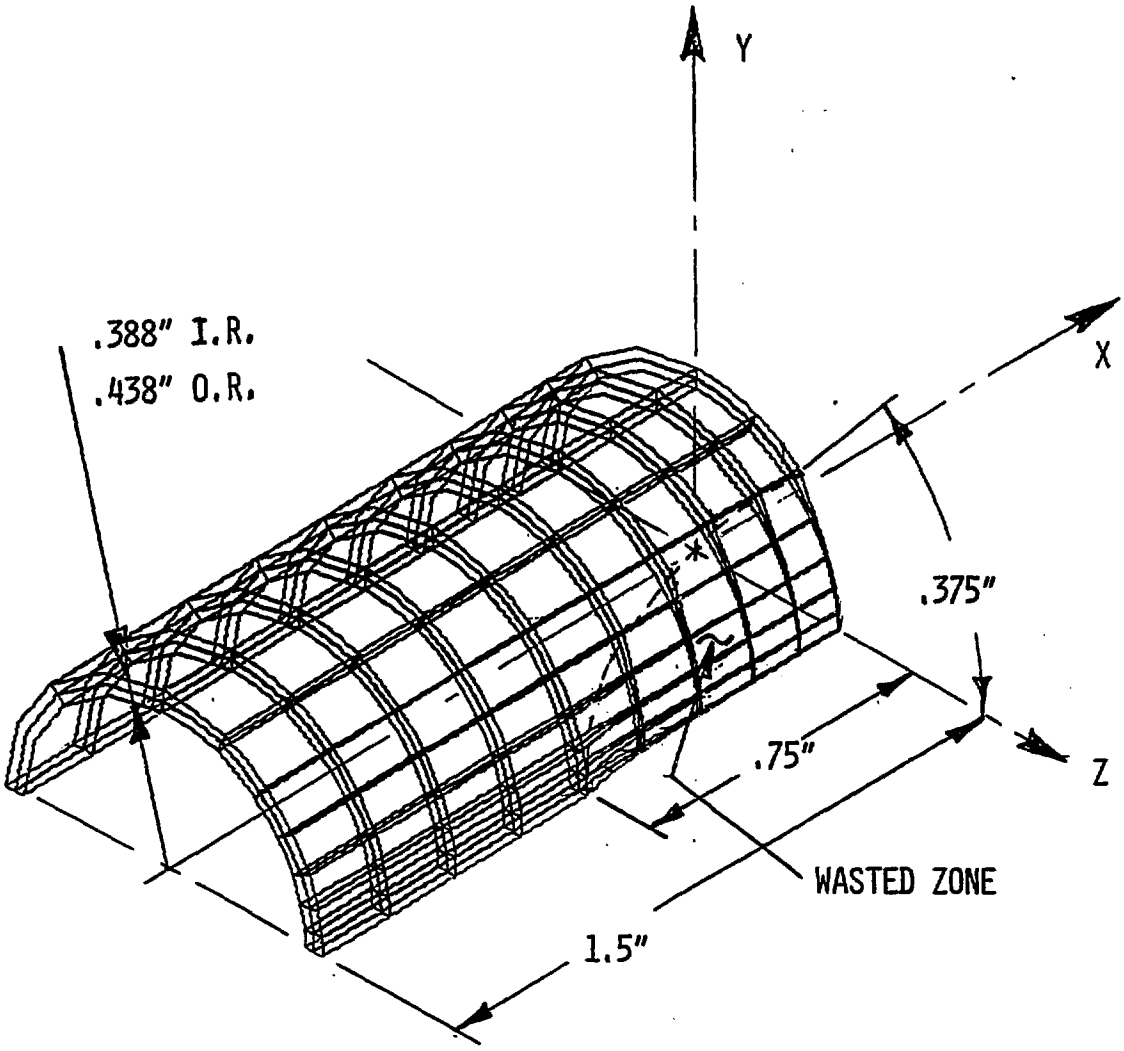

ELLIPTICAL WASTAGE IN STEAM GENERATOR TUBE

3-D GRID

FIGURE 6

80% THRU WALL ELLIPTICAL WASTAGE IN STEAM GENERATOR TUBE

PRESSURE VS STRESS AND STRAIN

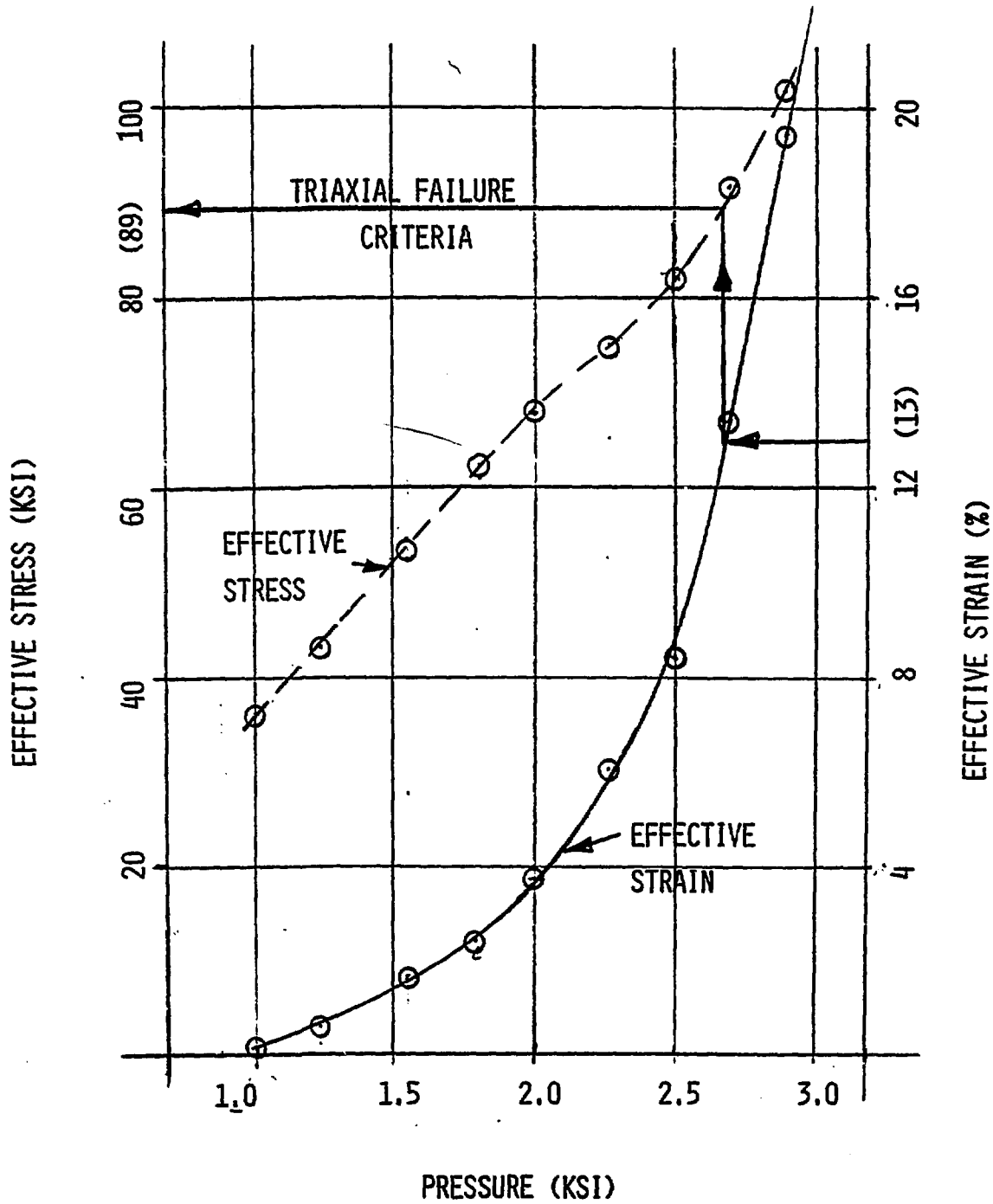

FIGURE 7

80% THRU WALL ELLIPTICAL WASTAGE IN STEAM GENERATOR TUBE

EFFECTIVE STRESS ON INNER SURFACE

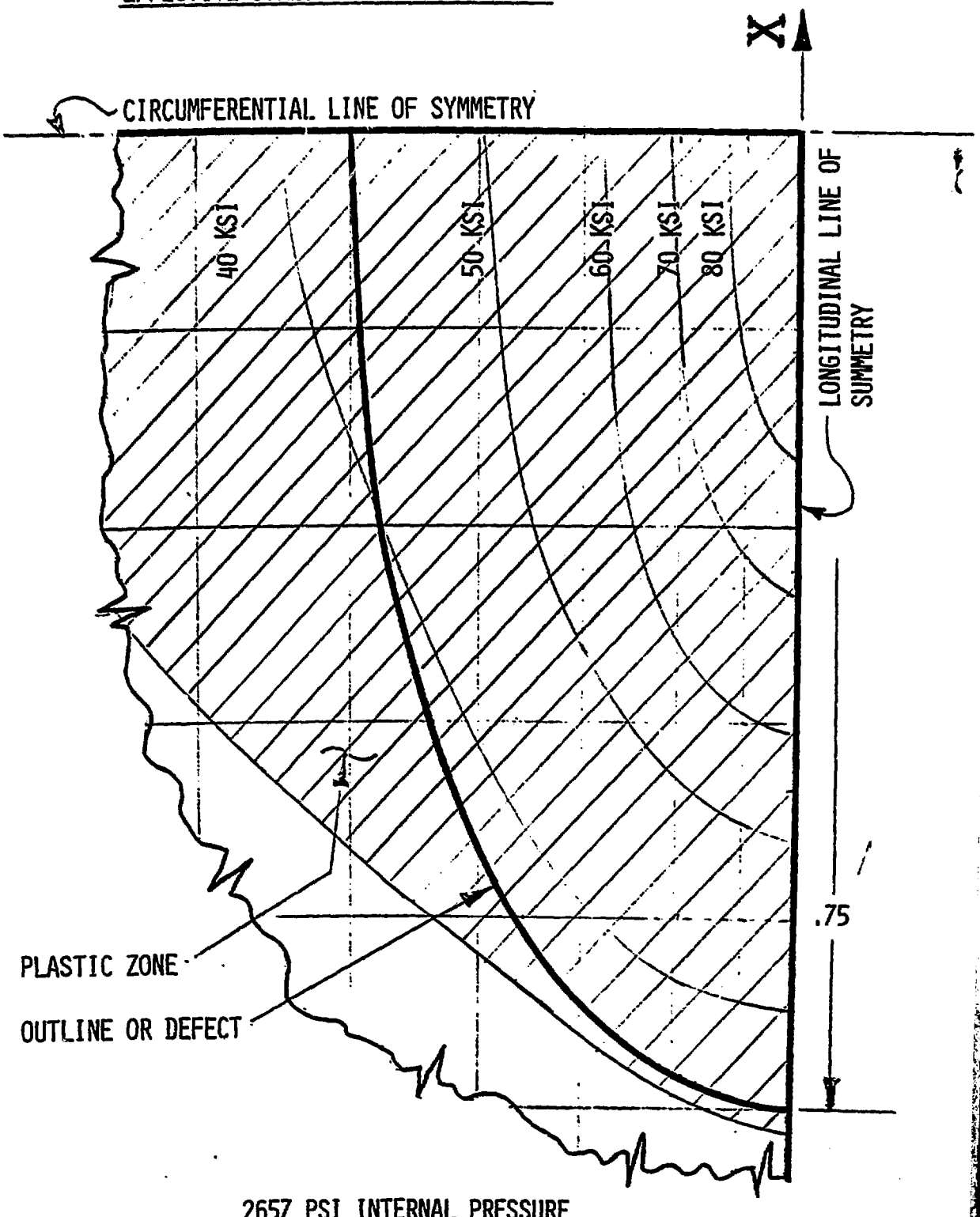

FIGURE 8

80% THRU WALL ELLEPTICAL WASTAGE IN STEAM GENERATOR TUBE

EFFECTIVE STRESS ON OUTER SURFACE

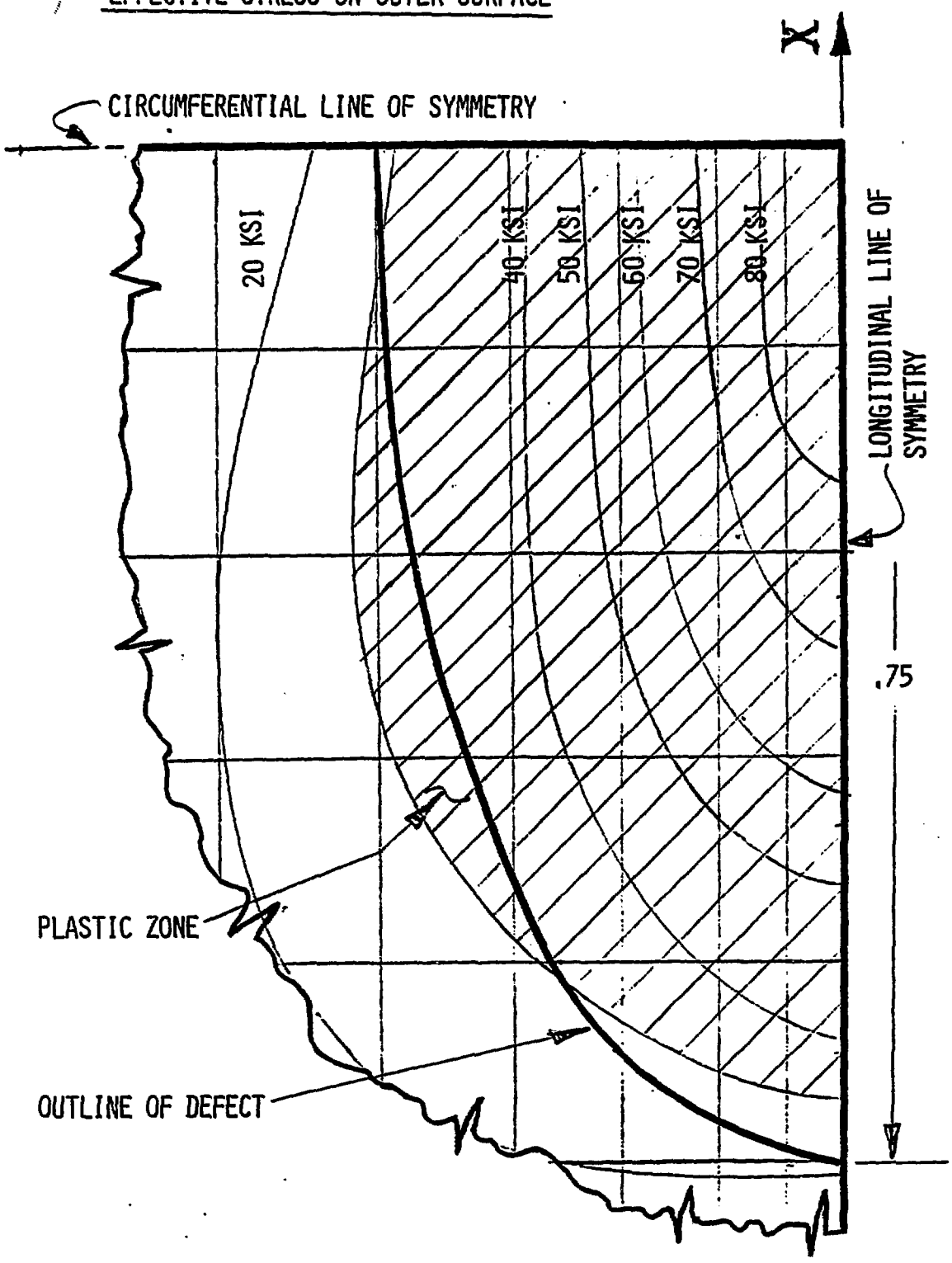

2657 PSI INTERNAL PRESSURE

FIGURE 9

80% THRU WALL ELLIPTICAL WASTAGE IN STEAM GENERATOR TUBE

RADIAL DEFLECTION AT VARIOUS PRESSURES

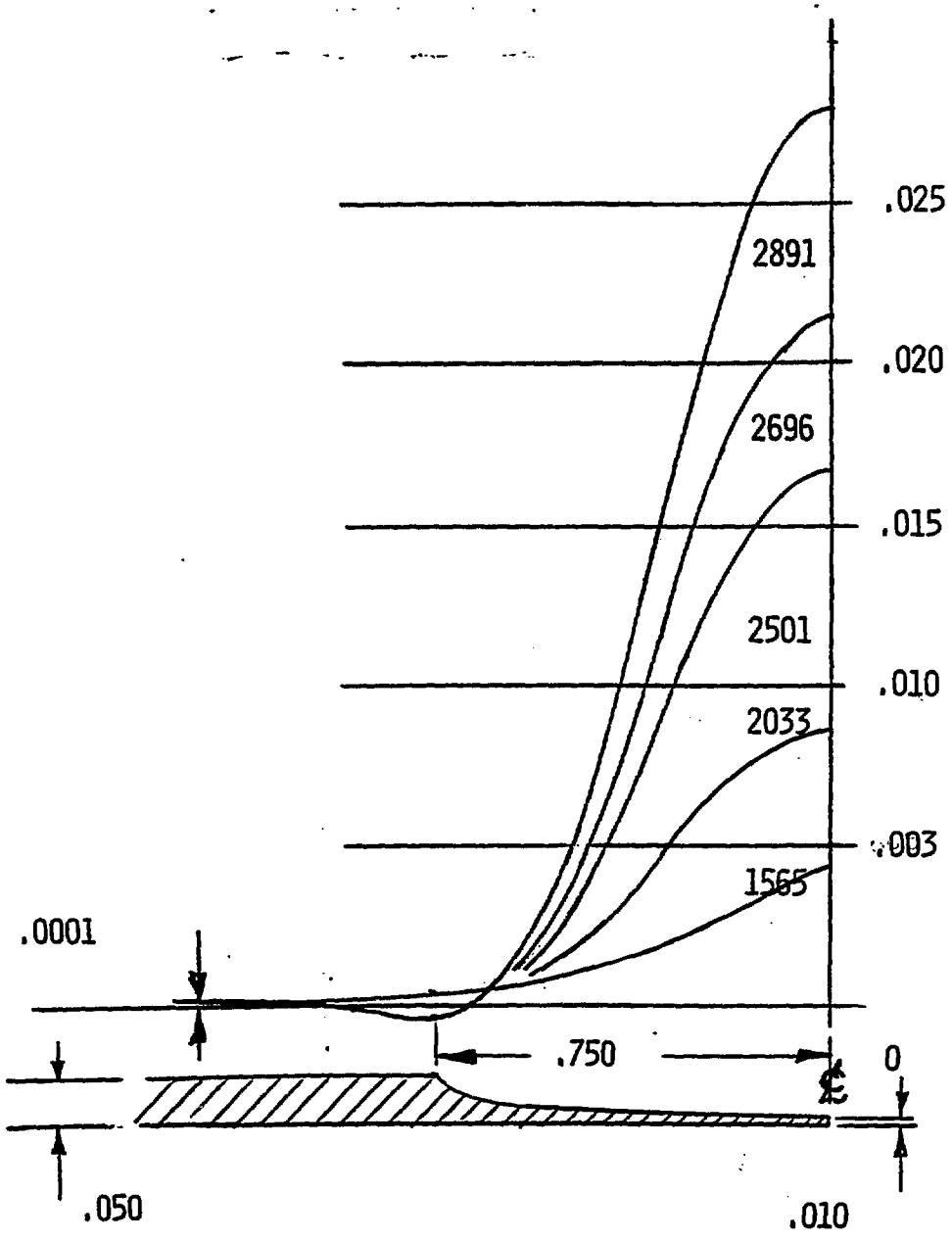

FIGURE 10

occur. A similar type of effect can also be expected to occur for the elliptical wastages under consideration herein. In view of the above, the results shown in Table 1 can be considered to be conservative with the degree of conservatism varying as per the discussion above.

From Table 1 it can be seen that a tube with a 50 percent wastage meets the margin of safety criteria outlined in the Regulatory Guide 1.121. In addition, if we take account of the three-dimensional strengthening effect, it is probable that the 60 percent wastage case also satisfies the criteria. Of course, for all cases, faulted conditions must be assessed separately.

Three-Dimensional Analysis of a Part-Thru Partial Arc Circumferential Crack

Figure 11 depicts the geometrical configuration of the flawed steam generator tube to be discussed, while Figure 12 shows the finite element grid used for the analysis. The mechanical properties of the tube are identical to those of the earlier analyses. For the case analyzed, involving only internal pressure, the presence of the crack does not appreciatively alter the failure pressure of the tube.

This can be clearly seen from Figures 13 through 16 which respectively depict the element integration point effective stresses for the inner and outer surfaces of the tube for internal pressures of 4300 psi (29.65 MPa) and 4800 psi (33.09 MPa). With the exception of a few points that have just become plastic at 3800 psi (26.20 MPa), the stress field on the inner surface of the tube is virtually uniform. This is even more true for the outer surfaces which are still completely in the elastic range. As can be seen from the latter two figures, the addition of approximately 500 psi (3.45 MPa) of internal pressure results in an almost uniform effective stress field for both the inner and outer surfaces with no

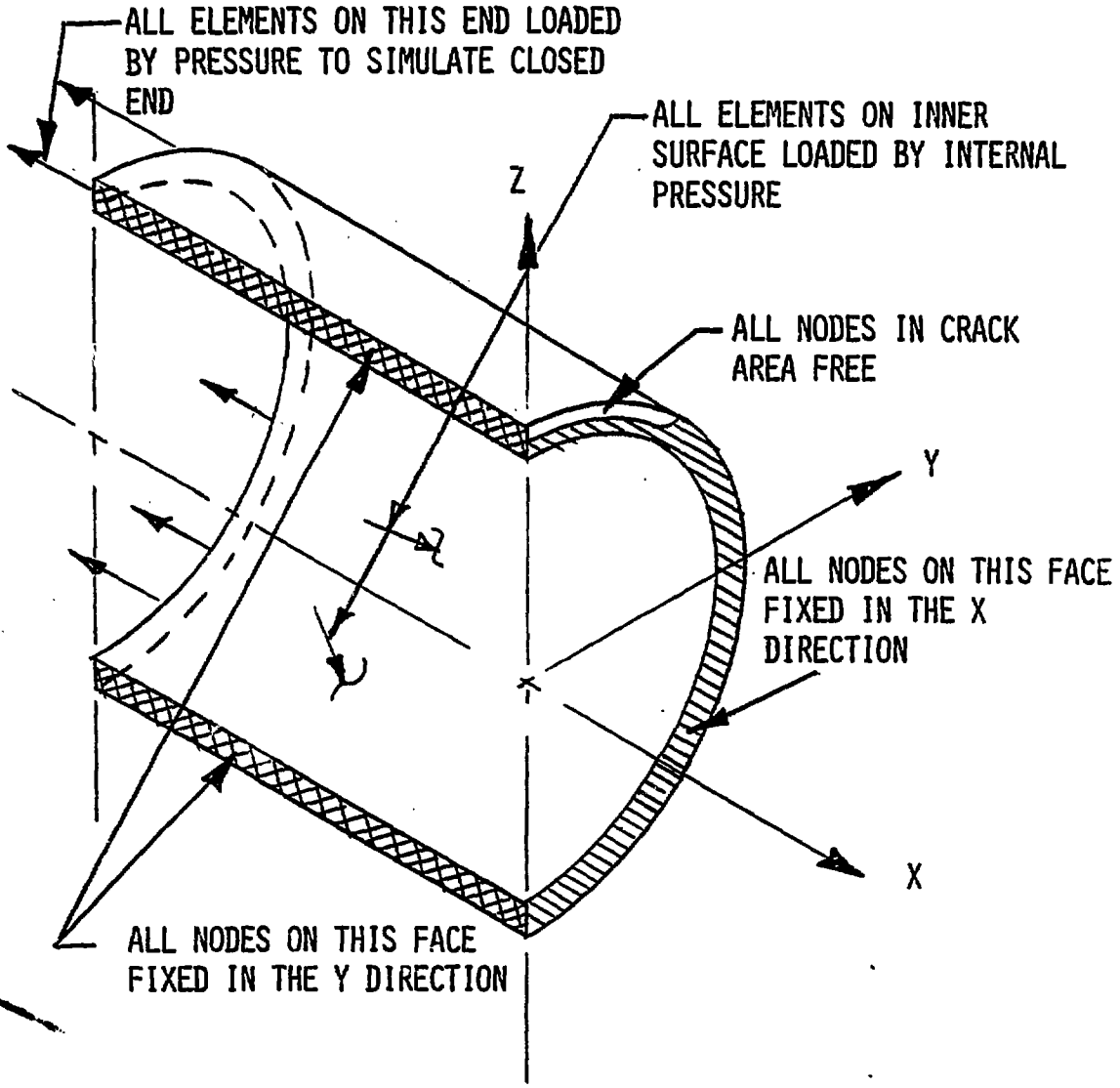

50% THRU WALL CIRCUMFERENTIALLY CRACKED STEAM GENERATOR TUBE LOADING AND RESTRAINTS

FIGURE 11

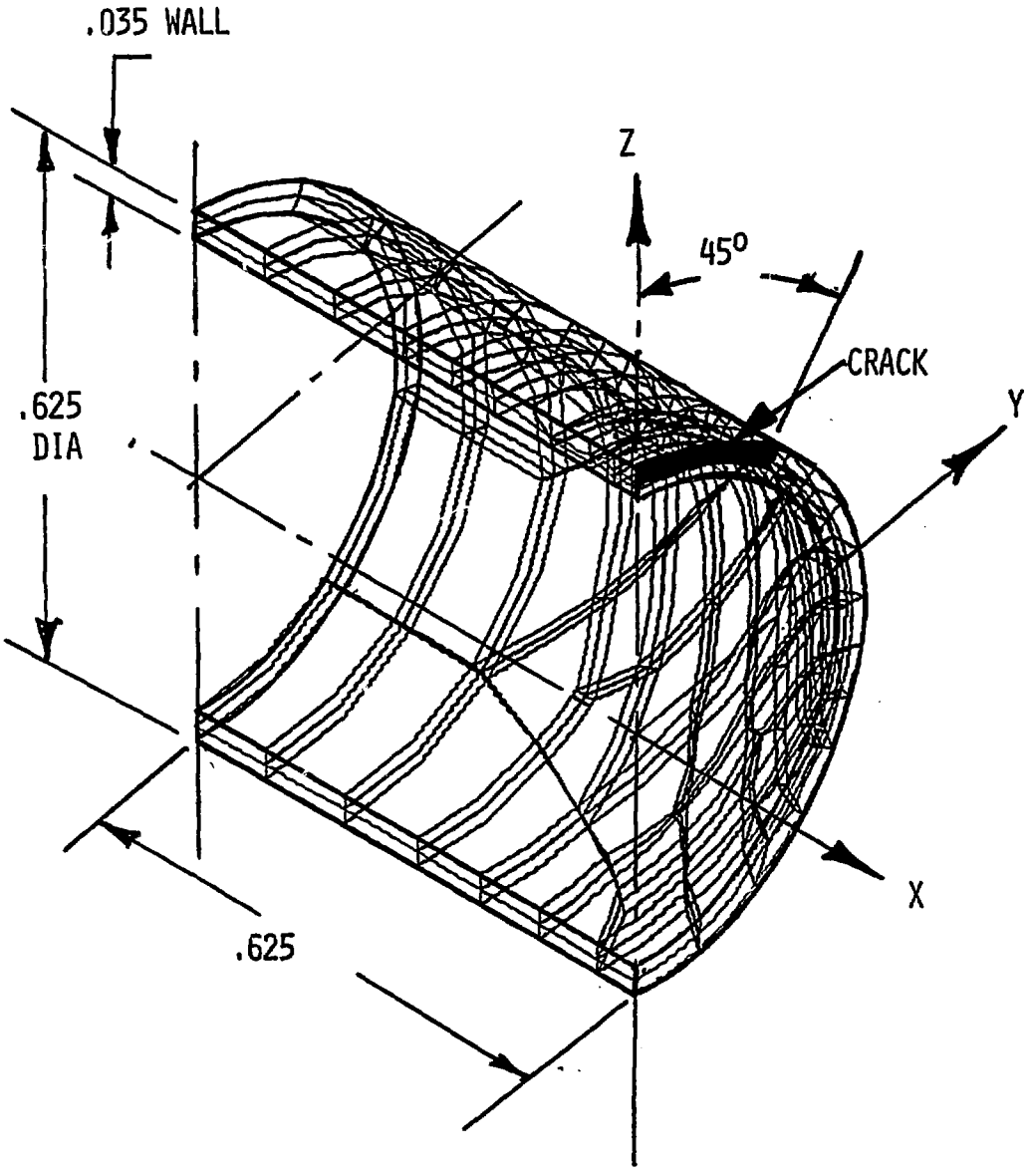

50% THRU WALL CIRCUMFERENTIALLY CRACKED STEAM GENERATOR TUBE

FINITE ELEMENT MODEL

FIGURE 12

50% THRU WALL CIRCUMFERENTIALLY CRACKED STEAM GENERATOR TUBE

EFFECTIVE STRESS AT 4300 PSI ON INNER SURFACE

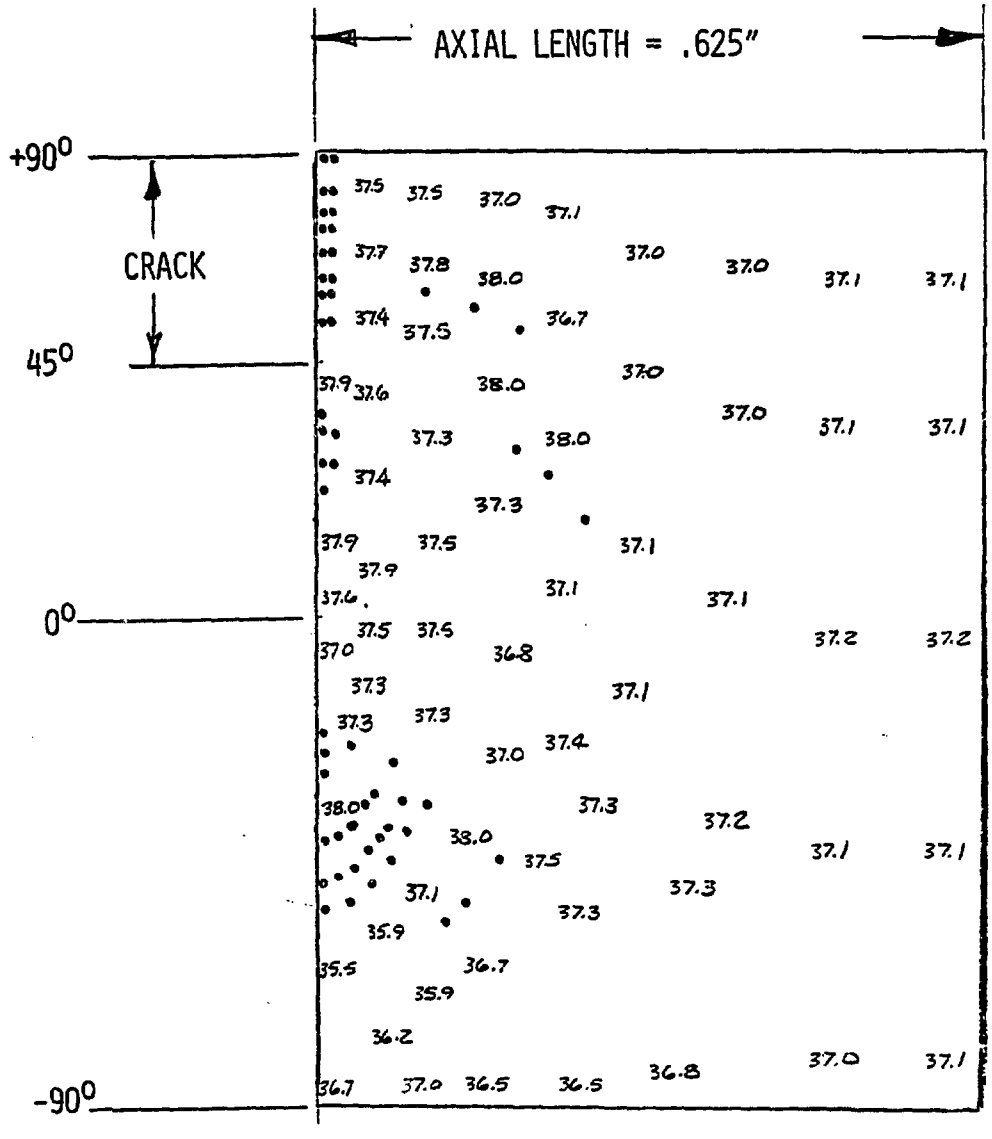

NOTE: ALL SURFACE INTEGRATION POINTS ARE ELASTIC EXCEPT THOSE INDICATED BY •

FIGURE 13

50% THRU WALL CIRCUMFERENTIALLY CRACKED STEAM GENERATOR TUBE

EFFECTIVE STRESS VALUES AT 4300 PSI ON OUTER SURFACE

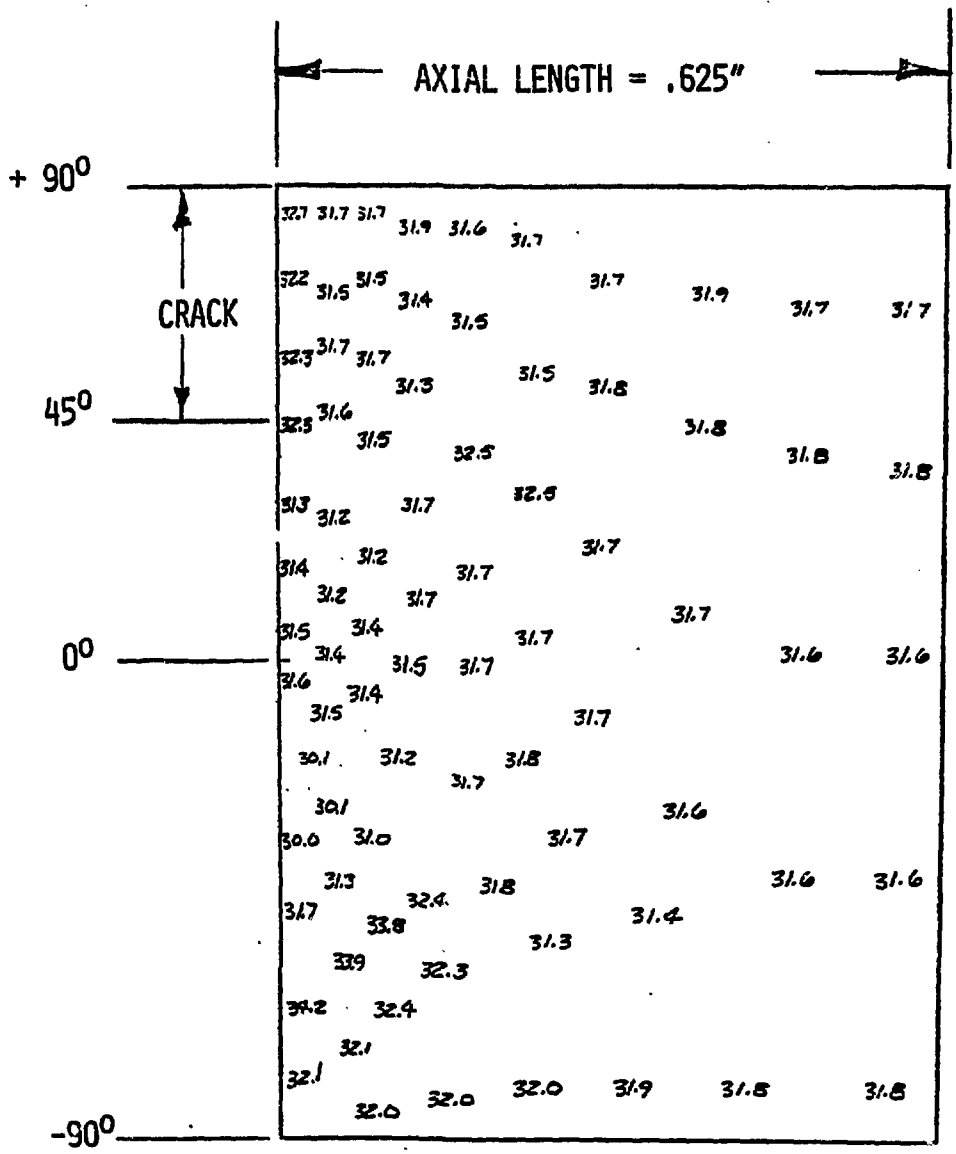

NOTE: ALL SURFACE INTEGRATION POINTS ARE ELASTIC

FIGURE 14

50% THRU WALL CIRCUMFERENTIALLY CRACKED STEAM GENERATOR TUBE

EFFECTIVE STRESS VALUES AT 4800 PSI ON INNER SURFACE

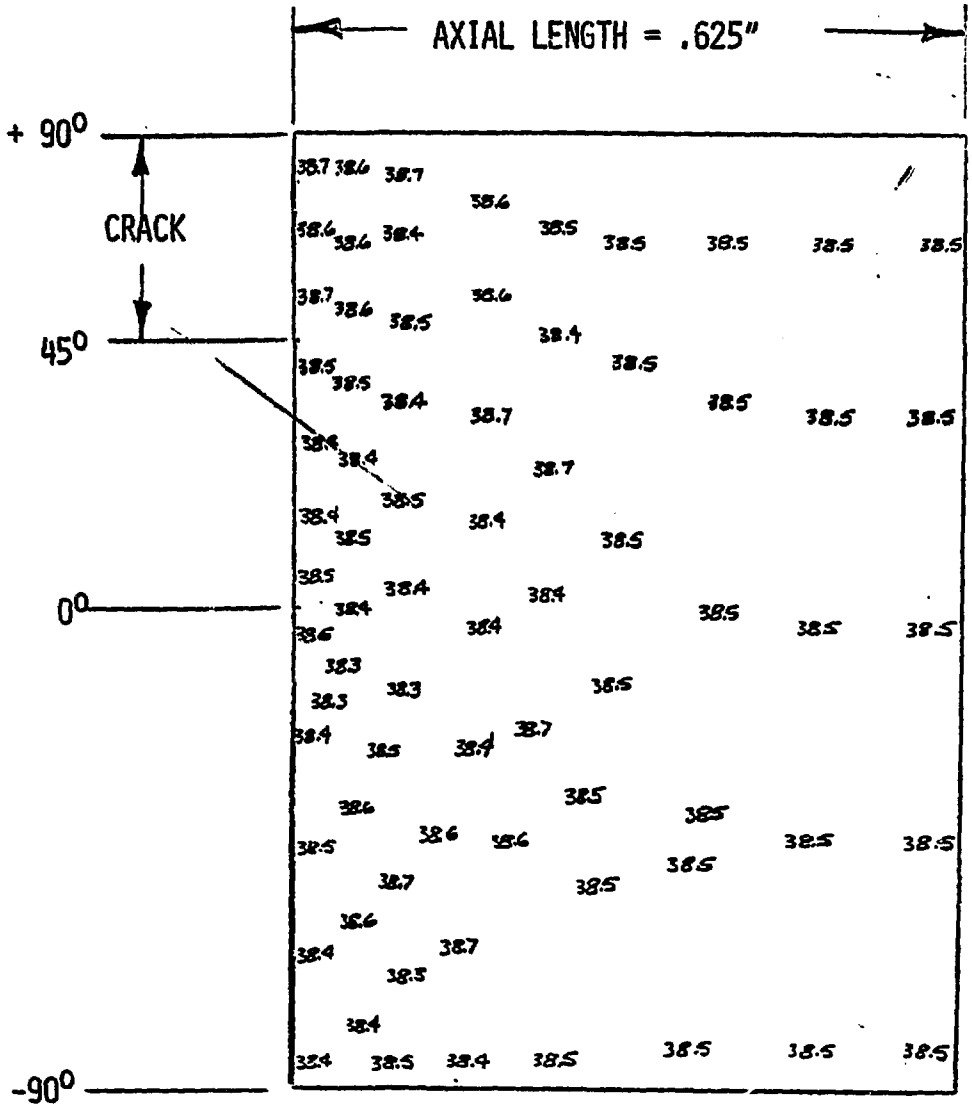

NOTE: ALL SURFACE INTEGRATION POINTS ARE PLASTIC.

FIGURE 15

50% THRU WALL CIRCUMFERENTIALLY CRACKED STEAM GENERATOR TUBE

EFFECTIVE STRESS VALUES AT 4800 PSI ON OUTER SURFACE

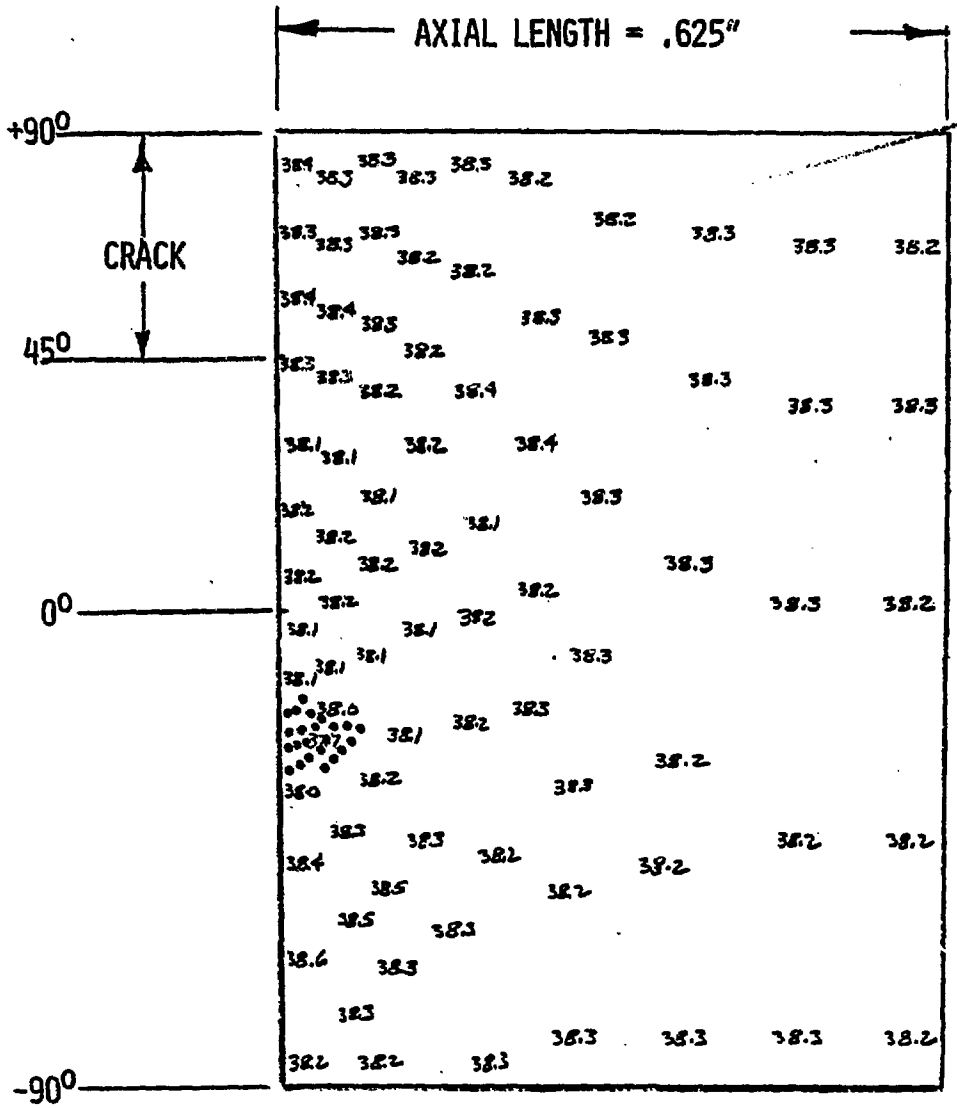

NOTE: ALL SURFACE INTEGRATION POINTS ARE PLASTIC EXCEPT THOSE INDICATED BY ●

FIGURE 16

appreciative stress riser in the region of the crack. The reason for this is that the predominant stress for this case is the hoop stress, which is only slightly effected by the crack. In fact, for the stress distribution of a tube under monotomic pressure the strain distribution is such that the crack does not open, thus, stress concentration effects are negligible. It is to be noted, however, that these findings would not apply if moment loadings act on the tube.

Analysis of Results for Seized Tubes

Figure 17 depicts schematically the tube and support plate configurations under study. The finite element idealization of the above configuration is shown in Figure 18, where axisymmetric finite elements were used. In view of the cyclic load considerations, the kinematic hardening rule is applied. The assumptions made for this problem are that the tube and the support plate are integrally connected and that due to symmetry, the outer edge of the plate is restrained in the horizontal direction.

The following cyclic loading sequence was applied: Pressure on the primary side goes from 0 to 2250 psi (15.510 MPa) while the pressure on the secondary side varies from 0 to 750 psi (5.171 MPa). Similarly and simultaneously, the temperature of the tube is increased uniformly from 70°F (21.10°C) to 620°F (326.67°C) while the plate temperature is increased from 70°F (21.10°C) to 560°F (293.3°C). The material properties for the tube and support plate were assumed to be similar with the exception that the coefficient of thermal expansion of the plate was $\alpha = 0.706 \times 10^{-5}$ in/in/°F (0.127×10^{-4} cm/cm/°C) while that of the tube was $\alpha = 0.785 \times 10^{-5}$ in/in/°F (1.141×10^{-4} cm/cm/°C. The values assumed for the elastic modulus, the tangent

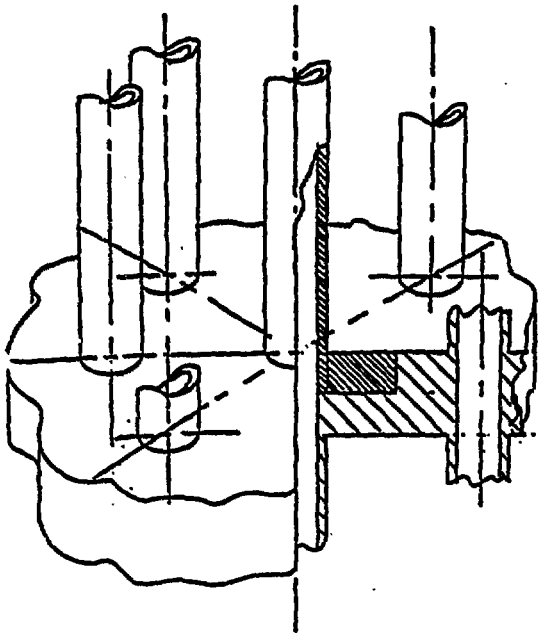

SCHEMATIC VIEW OF SUPPORT PLATE
AND TUBE CONFIGURATION

FIGURE 17

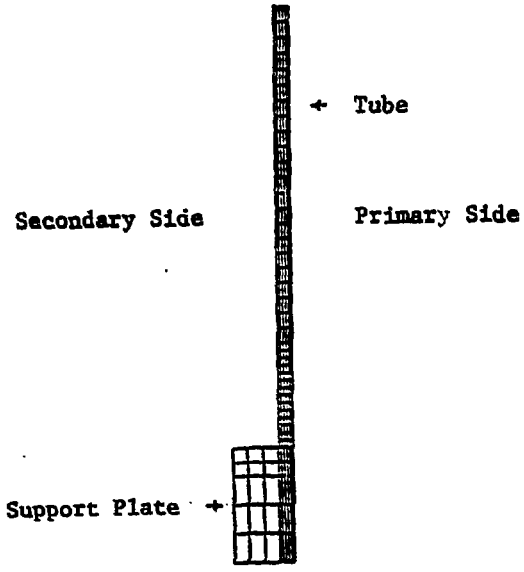

THE FINITE ELEMENT GRID IDEALIZATION OF THE SUPPORT PLATE AND THE TUBE

FIGURE 18

modulus, the yield stress, and poisson's ratio are respectively: $E = 30 \times 10^6$ psi (20.68×10^4 MPa); $E_t = 25.6 \times 10^4$ psi (17.65×10^2 MPa); $\sigma_y =$ 38,000 psi (262.0 MPa); and $\nu = .3$.

Figures 19 and 20 show the calculated deformed shape of the tubes after 10, 20, and 30 cycles at full load and zero load respectively. Figures 21 and 22 depict results of hoop stress and strain at the inner and outer radius of the tube at full load vs. the number of cycles while Figures 23 and 24 show the results when the temperature and pressure loads are reduced to zero. The stress-strain history points for points A and B located at the inner and outer radius are shown respectively in Figures 25 and 26.

In evaluating the results shown in the above-mentioned figures, it becomes apparent that for the boundary conditions and material assumptions made in this analysis, there is a continuous plastic zone and plastic strain growth for each of the loading cycles considered. It is to be noted, however, that the plastic growth rate per cycle is decreasing. Thus, two possibilities exist, that is, plastic action will cease at some subsequent cycle or plastic growth will continue indefinitely. In the first case the designer will be faced with a fatigue problem while for the latter case the design will fail by ratcheting. In neither case can the problem be considered to be that of a simple shakedown situation.

As mentioned, simplified approximations were made for the seized tube analyses. Firstly, the assumptions of identical yield strengths and tangent moduli for the tube and plate may not fit all applications. Generally speaking, if the plate material is softer than the tube material, a greater

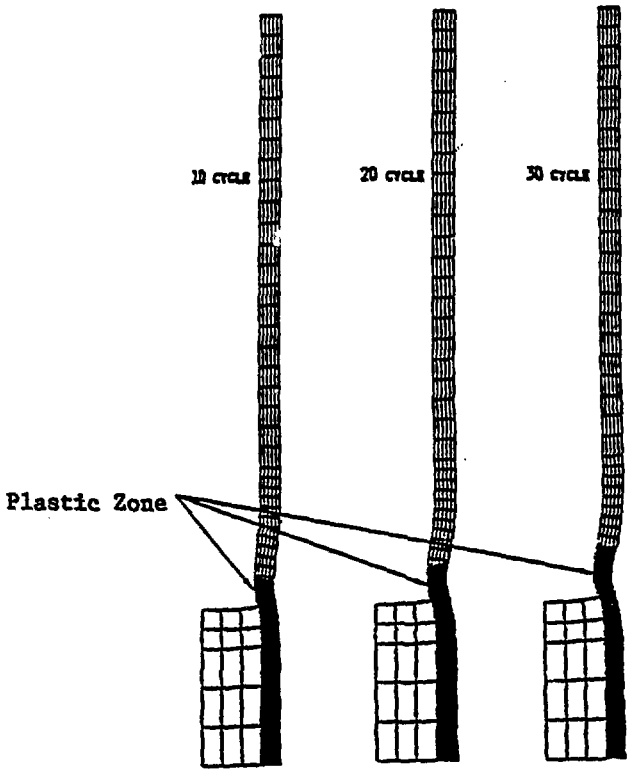

THE PROPAGATION OF PLASTIC ZONE AFTER 10, 20, AND 30 CYCLES AT FULL LOAD

FIGURE 19

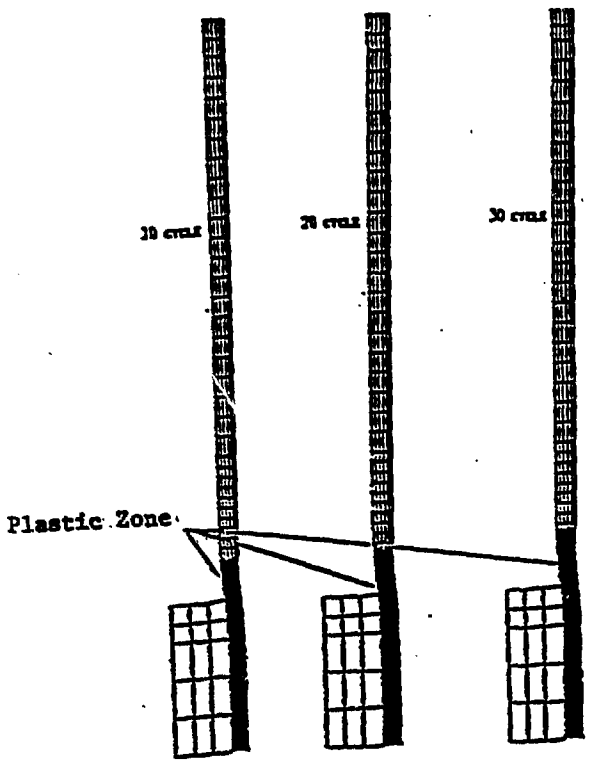

THE PROPAGATION OF THE PLASTIC ZONE AFTER 10, 20, AND 30 CYCLES AT NO LOAD

FIGURE 20

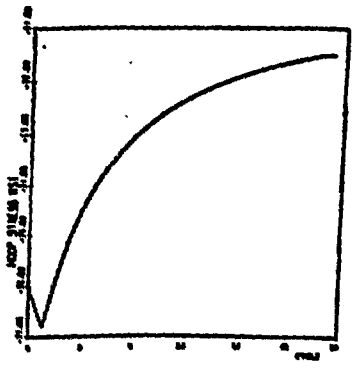

HOOP STRESS AT THE INNER RADIUS AT FULL LOAD VS. CYCLE

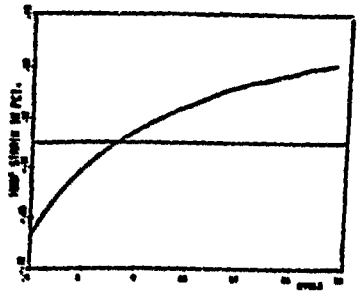

HOOP STRAIN AT THE INNER RADIUS AT FULL LOAD VS. CYCLE

FIGURE 21

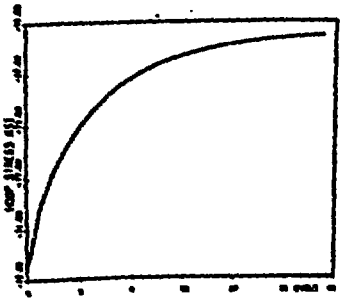

HOOP STRESS AT OUTER RADIUS AT FULL LOAD VS.CYCLE

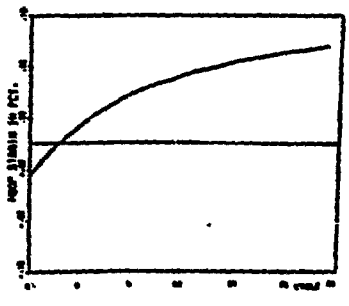

HOOP STRAIN AT OUTER RADIUS AT FULL LOAD VS. CYCLE

FIGURE 22

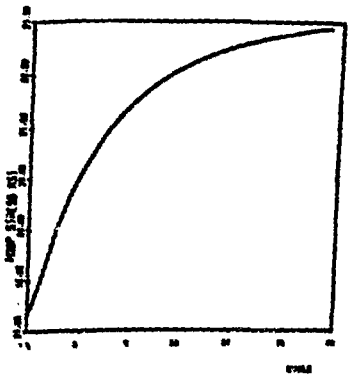

HOOP STRESS AT INNER RADIUS AT NO LOAD VS. CYCLE

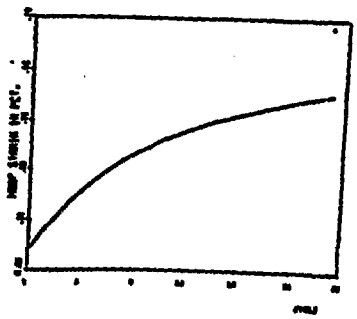

HOOP STRAIN AT INNER RADIUS AT NO LOAD VS. CYCLE

FIGURE 23

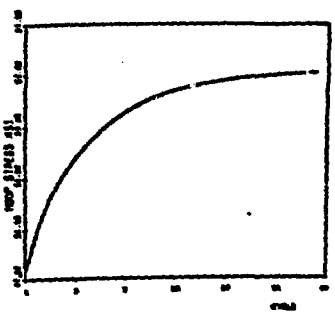

HOOP STRESS AT OUTER RADIUS AT NO LOAD VS. CYCLE

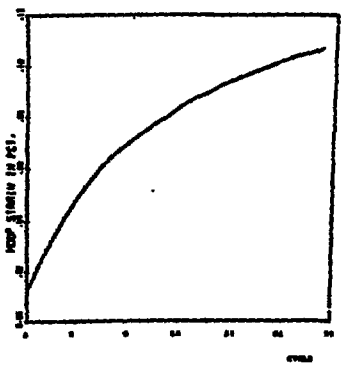

HOOP STRAIN AT OUTER RADIUS AT NO LOAD VS. CYCLE

FIGURE 24

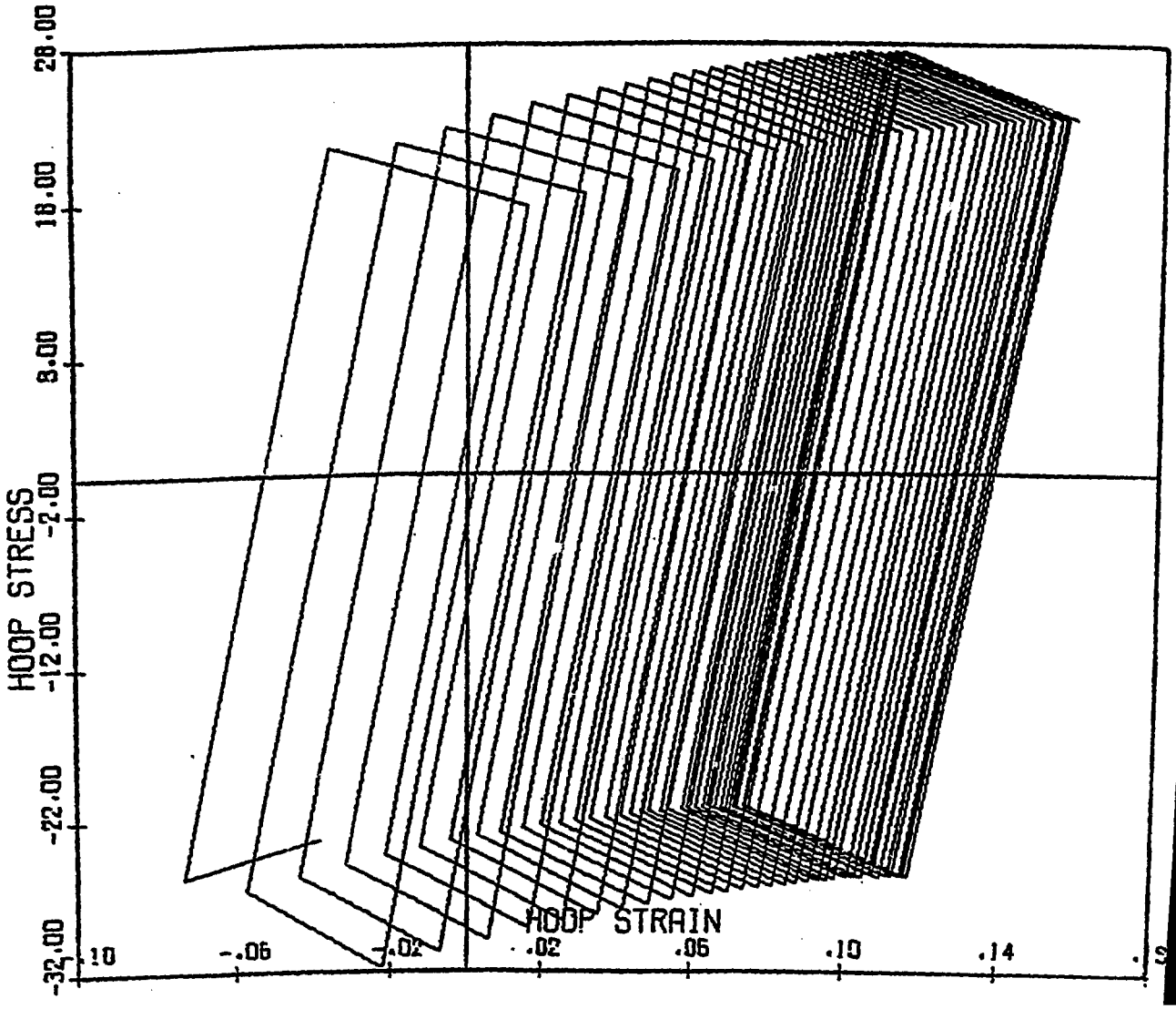

STRESS-STRAIN HISTORY AT THE INNER SURFACE

FIGURE 25

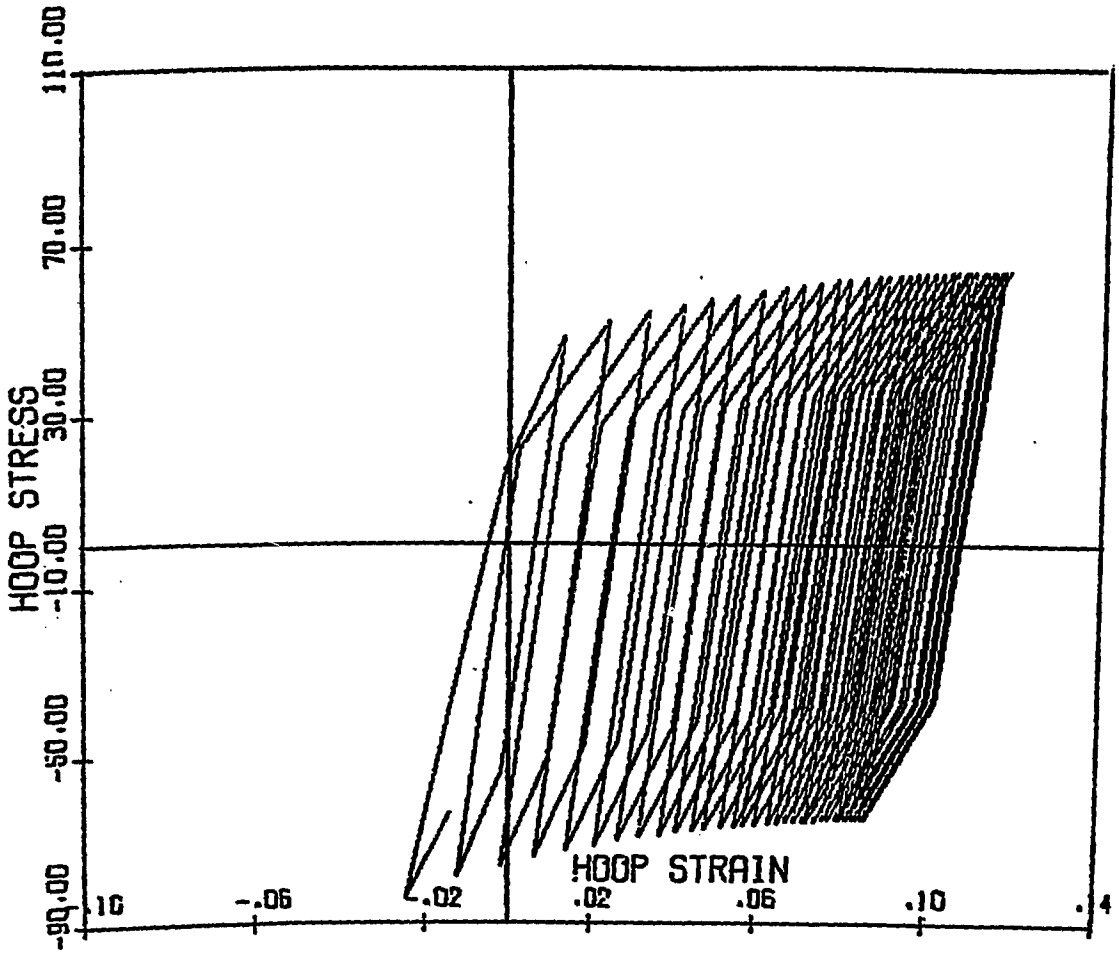

STRESS-STRAIN HISTORY AT THE OUTER SURFACE

FIGURE 26

tendency towards a fatigue situation would exist. Alternatively, if the plate is stiffer, then the potential for ratcheting would be greater.

Another major assumption made was that the plate and the tube were integrally connected. In the actual situation the tube may break away from the support plate during each cycle (during unloading). If this occurs the possibility of progressive "crud" build-up exists, thus progressively decreasing the support plate hole diameter. When this occurs, ratcheting failure is most probable since the plastic strain per cycle will be higher than the case considered herein. This case should be treated analytically since the method for carrying out this type of analysis does exist.

Finally, the possibility of flaws in the vicinity of the high stress regions can strongly alter the behavior of the system. These effects together with experimental verification, using physical models, should be undertaken. This only pertains to normal condition, and not upset.

Conclusions

Two and three-dimensional evaluations of steam generator tubes having denting, wastage, and circumferential and longitudinal cracks have been made. From these evaluations it can be inferred that the two-dimensional analyses will provide conservative estimates of the burst pressure for cases involving pressure loadings only. The degree of conservatism for cracked wasted configurations is a function of the defect length, depth, and shape; furthermore, for denting problems the axisymmetric analysis results are as good as the boundary conditions and the material property assumptions made. In addition the possibility of flaws associated with the denting phenomena can strongly alter the present calculated results.

REFERENCES

1. Morgan, E. P., Pement, F. W., Esposito, J. N., and Aspden, R. G., "Examination of Denting and Characterization of Associated Materials in the Plate-Tube Intersections of Westinghouse Nuclear Steam Generators," CORROSION/77, Corrosion Research Conference, San Francisco, California, March 1977.

2. Economy, G., Wootten, M. J., Rebler, A. R., and Lindsay, W. T., "Laboratory Investigations Related to Denting in Nuclear Steam Generators," CORROSION/77, Corrosion Research Conference, San Francisco, California, March 1977.

3. Van Rooyan, D., "Corrosion in the Nuclear Power Industry - An Overview," CORROSION/77, Corrosion Research Conference, San Francisco, California, March 1977.

4. Domain, H. A., Emanuelson, R. H., Katz, L., Sarver, L. W., and Theus, G. J, "Effect of Microstructure on Stress Corrosion Cracking of Alloy 600 in High Purity Water," CORROSION/76, Preprint No. 99, Houston, Texas, March 1976.

5. Schenk, H. J., "Tube Defects in KWO Steam Generators and Results of Their Investigations," CORROSION/75, Preprint No. 115, Toronto, Canada, 1975.

6. United States Nuclear Regulatory Commission, "Basis for Plugging Degraded PWR Steam Generator Tubes," Regulatory Guide 1.121, August 1976.

7. Reich, M., Chang, T. Y., Prachuktam, S., Bezler, P., and Gardner, D., "Determination of Burst Pressures for Cracked Steam Generator Tubes," BNL No. 22076, ASME 77-PUP-31, Presented at the ASME Energy Technology Conference, Houston, Texas, September 1977.

8. Prachuktam, S., Reich, M., Gardner, D., and Chang, T. Y., "NFAP - The Nonlinear Finite Element Analysis Program - User's Manual (1977 Version)," In preparation.

9. Davis, E. A. and Connelley, F. M., Stress Distribution and Plastic Deformation on Rotating Cylinders of Strain-Hardening Material, Journal of Applied Mechanics, Trans ASME Vol 26, 1959, pp 25-30.

10. Cooper, W. E., Significance of the Tensile Test to Pressure Vessel Design Welding, Journal Research Supplement, January 1957.

FAILURE ANALYSIS OF STEAM GENERATOR TUBES WITH DENTED AND WASTAGE CONFIGURATIONS

M. REICH, S. PRACHUKTAM, D. GARDNER, H. GORADIA, P. BEZLER, K. KAO

Distribution List:

Dr. Robert J. Bosnak, Chief
Mechanical Engineering Branch
U. S. Nuclear Regulatory Commission
Division of Systems Safety
Washington, DC 20555

Dr. Lawrence Shao
Division of Operating Reactors
U. S. Nuclear Regulatory Commission
Washington, DC 20555

Dr. Mark Hartzman
Mechanical Engineering Branch
Division of Technical Review
U. S. Nuclear Regulatory Commission
Washington, DC 20555

Dr. J. P. Knight
Division of Systems Safety
Office of Nuclear Reactor Regulation
Mail Stop 1014 B
U. S. Nuclear Regulatory Commission
Washington, DC 20555

Dr. Boen-Dar Liaw
Division of Operating Reactors
U. S. Nuclear Regulatory Commission
Washington, DC 20555

Dr. J. Rajan
Mechanical Engineering Branch (10 Copies)
U. S. Nuclear Regulatory Commission
Washington, DC 20555

Dr. E. Sullivan
Mechanical Engineering Branch
U. S. Nuclear Regulatory Commission
Washington, DC 20555

BNL Distribution List:

T. O'Hare

W. Kato

H. Kouts

D. Van Rooyen

J. Weeks